Technical Note

ISSN 1997-1400 Int. J. Pavement Res. Technol. 6(6):773-777

Fracture Behavior of Asphalt Pavement with Cracked Base Course under Low Temperature

Yu Chen[1+] and Chuanchao Zheng[1]

Abstract: Low temperature cracking is a distress mode of particular concern for asphalt pavements in cold regions. Traditionally, research regarding pavement low temperature cracking has mainly focused on surface-initiated transverse cracking. However, cracks in underlying base course can reflect through asphalt pavement layers under thermal stresses. In this study, a new approach (refined mesh) to describe crack tip stress singularity was introduced to study the low temperature cracking behavior with cracked base course using the Finite Element Method (FEM). Fracture toughness of one asphalt mixture that is commonly used in the northern part of China was measured under three temperatures, 0˚C, -10˚C and -20˚C. Sensitivity analysis was performed on stress intensity factor at crack tip to determine critical factors on surface course cracking behavior. Meanwhile, cracking behavior of surface course was evaluated by comparison between stress intensity factors at crack tip and mixture fracture toughness. Results indicated that surface course thickness has little effect on stress intensity factor at crack tip, and that the crack propagation in asphalt pavement surface course can be divided into two stages, stable and unstable.

DOI: 10.6135/ijprt.org.tw/2013.6(6).773

***Key words**: Asphalt pavement; Fracture toughness; Low temperature cracking; Stress intensity factor.*

Introduction

Low temperature cracking is a major distress mode for asphalt pavements in cold climates. Traditionally, research regarding pavement low temperature cracking has mainly focused on surface-initiated transverse cracking with various lengths and widths [1-5]. However, little research has been done on reflection cracking caused by thermal stresses when the underlying base course was cracked. Fracture mechanics was commonly used to characterize pavement cracking because traditional solid mechanics only ensures either stress or strain remains below the design limits, namely the pavement strength. However, flaws or defects, which are inevitable in all materials, can greatly reduce the pavement stress or strain bearing capacity. To evaluate crack initiation and propagation, the Finite Element Method (FEM) was often employed to calculate stress intensity factors at crack tips. Most FEM approaches use singular elements to capture crack tip stress singularity, which often involves tedious and non-straightforward work [6-8]. In this study, a new approach using refined regular elements at crack tip to describe stress singularity was proposed and verified using laboratory testing results.

Model Development and Verification

To capture stress singularity at crack tip, finite element size near crack tip is usually selected to be 1/1,000 to 1/10 of the crack length. In this study, 1mm×1mm element size (1/10 of 10 mm notch) was chosen. The FEM model of half the test specimen is shown in Fig. 1. All materials in the model were assumed to be homogenous, isotropic, and elastic. Half of the peak load employed in the actual testing was applied on the model (See Fig. 1). Plane stress quadrilateral isoparameter elements with refinement near crack tip were used in the analysis to capture the crack tip region stress distribution. The stress intensity factor can be calculated using Eq. (1). Stress intensity factor K_I for three points with distances 2 mm, 3 mm, and 4 mm from crack tip were calculated and used to predict the stress intensity factor at crack tip as presented in Fig. 2.

$$K_I = \sigma_x \times \sqrt{2\pi r} \quad (1)$$

where,

K_I = stress intensity factor, $MPa\sqrt{mm}$

σ_x = tensile stress perpendicular to crack, MPa

r = polar coordinate with respect to crack tip as origin, mm

Model Verification

Three point bending beam tests were conducted on one type of asphalt mixture under three temperatures 0˚C, -10˚C, and -20˚C. The mixture is commonly used in the northern part of China and identified as AC13-110 [9]. The dimension for beam specimens is 50mm×50mm×250mm and the loading rate is 50mm/minute. All specimens are pre-notched to 10mm deep. To reduce specimen to

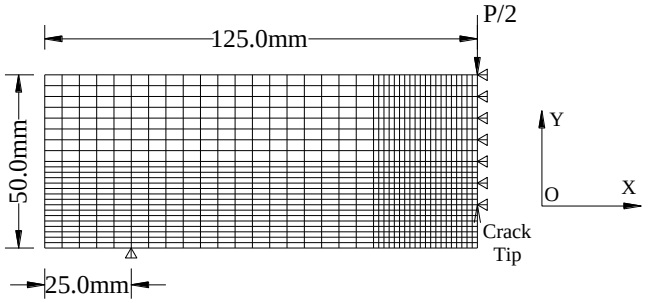

Fig. 1. 1/2 FEM Model of Test Specimen.

[1] Highway School, Chang'An University, Xi'An, China 710064.

[+] Corresponding Author: E-mail chenyu1123@gmail.com

Note: Submitted October 17, 2012; Revised February 23, 2013; Accepted March 31, 2013.

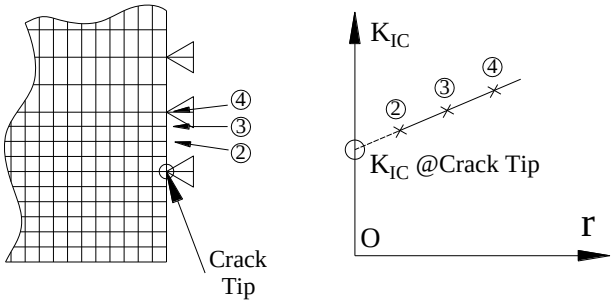

Fig. 2. Calculation of Fracture Toughness K_{IC}.

Table 1. Peak Load Under 0˚C, -10˚C and -20˚C.

Number	00-1	00-2	00-3	00-4	00-5
P(N)	2779	2854	2620	2550	2925
Number	10-1	10-2	10-3	10-4	10-5
P(N)	3054	3361	3134	3057	2771
Number	20-1	20-2	20-3	20-4	20-5
P(N)	2933	2463	3018	2337	2835

Note: 00=0˚C; 10= -10˚C; 20= -20˚C.

specimen variability, 5 specimens for each temperature were tested,and peak load results are presented in Table 1. Moduli of HMA for the numerical analysis were measured at three temperatures, 0˚C, -10˚C, and -20˚C, and were determined to be 1,807 MPa, 4,196 MPa, and 7,959 Mpa, respectively. According to Chen [10], fracture toughness for three point bending beam can be calculated using Eq. (2). Fracture toughness results from both FEM analysis by Eq. (1) and three point beam tests by Eq. (2) are presented in Table 2. As can be seen in Table 2, there is little difference between numerical and testing results on fracture toughness, which indicates that element refinement is an effective approach to capture the stress singularity near the crack tip.

$$K_{IC} = M \Big/ \left[B \times^{3/2} \sqrt{W}\right]\left[7.31 + 0.21 \times \sqrt{S/W - 2.9}\right] \sec\left(\frac{\pi a}{2w}\right) \sqrt{\tan\left(\frac{\pi a}{2w}\right)} \quad (2)$$

where,
B = Specimen width, mm
M = P×S/4, N×mm
P = Peak load during beam test, N
S = Distance between points of support for the beam, mm
W = Specimen height, mm
a = Notch length, mm

Pavement Structure Model under Thermal Stresses

As stated earlier, research regarding pavement low temperature cracking has mainly focused on surface-initiated transverse cracking with various lengths and widths. However, little research has been done on reflection cracking caused by thermal stresses when the underlying base course is cracked. In this section, one half two-dimensional pavement structure model, as shown in Fig. 3, was created to study the reflection cracking behavior under thermal stresses with cracked base course. All materials in the model were assumed to be homogenous, isotropic, and elastic. Plane stress quadrilateral isoparameter elements were used in this analysis. Parameters for thermal stress analysis are presented in Table 3. It should be noted that modulus of surface course mixture were measured at three temperatures, 0˚C, -10˚C, -20˚C, whereas the rest of the material properties are assumed to be constant with temperature.

Temperature boundary conditions are presented in Table 4 and structural boundary conditions of pavement structure are as follows,

- At $Y = -(h_1 + h_2 + h_3 + h_4)$, $u_Y = 0$ and $u_X = 0$, namely no movement allowed in either direction at the bottom of the subgrade; u_Y = displacement in y direction, u_X = displacement in x direction.
- At X = 0 in the range of $-(h_1 - 3mm) \leqq Y \leqq 0$ and $-(h_1 + h_2 + h_3 + h_4) \leqq Y \leqq -(h_1 + h_2)$, $u_X = 0$, namely no horizontal translation allowed in this range. Here the crack was assumed to propagate 3mm into the asphalt surface course to keep material continuity during the crack propagation progress. It should be noted that there is no constrain in the range of

Table 2. Numerical and Testing Results of Fracture Toughness.

Number	Numerical Results	Average	Testing Results	Average	Difference
00-1	32.114		32.904		
00-2	32.805		33.618		
00-3	29.486	31.439	30.243	32.221	-2.43%
00-4	29.274		29.963		
00-5	33.518		34.375		
10-1	36.068		36.945		
10-2	37.815		38.953		
10-3	35.63	35.399	36.468	36.323	-2.54%
10-4	35.588		36.527		
10-5	31.892		32.725		
20-1	35.148		36.066		
20-2	27.875		28.598		
20-3	34.188	31.181	34.974	31.959	-2.43%
20-4	26.913		27.565		
20-5	31.783		32.591		

Note: 00= 0˚C; 10 = -10˚C; 20 = -20˚C.

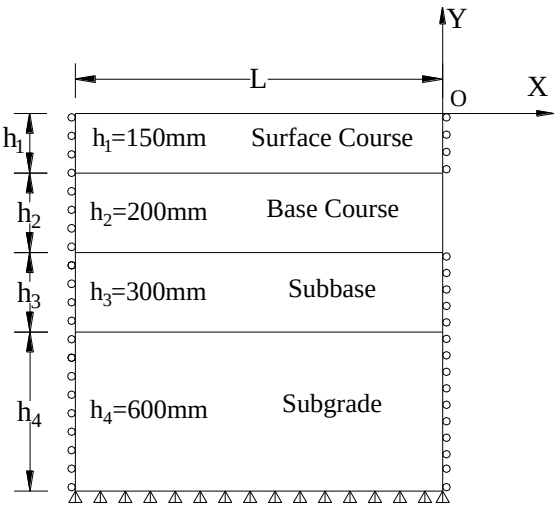

Fig. 3. Half Pavement Structural Model (Two Dimensional).

Table 3. Parameters for Thermal Stress Analysis [11].

Number	Modulus (MPa)	Poisson' Ratio	α (/˚C)	λ (W/(m•˚C))
Surface Course	E_1= 1807	μ_1= 0.25	α=3e-5	λ_1= 1.2
Base Course	E_2= 1000	μ_2= 0.25	α=1e-5	λ_2= 1.3
Subbase	E_3= 500	μ_3= 0.25	α_3=1.5e-4	λ_3= 1.3
Subgrade	E_4= 50	μ_4= 0.35	α_4=5e-4	λ_4= 1.5

Note: α = coefficient of thermal contraction; λ = coefficient of thermal conductivity; E_1= 1807 (0˚C), E_1= 4196 (-10˚C) E_1= 7959 (-20˚C).

Table 4. Temperature Boundary Conditions.

Temperature (˚C)	0		-10		-20	
Y	Temp	Tref	Temp	Tref	Temp	Tref
0	0	15	-10	5	-20	0
- h_1	5		-5		-15	
- (h_1+h_2+h_3)	10		0		-5	
- (h_1+h_2+h_3+h_4)	15		5		0	

Note: Tref = Reference temperature.

$-(h_1+h_2) \leqq Y \leqq -(h_1-3\ mm)$, which represents cracked base course.

- At X = – L, u_X = 0, namely no horizontal translation on the symmetric plane. L is half the thermal cracking space. Crack tip stress distribution was found to be identical for L = 4 m, 8 m and 12 m; thus, L = 4 m was used in this analysis to save computer run-time.

Sensitivity Analysis of Stress Intensity Factors Under Thermal Stresses

In this section, analysis was performed on pavement structure as shown in Fig. 3, with structural and temperature boundary conditions as stated in the previous section. The effects of surface thickness, surface modulus, coefficient of thermal contraction for surface course, coefficient of thermal contraction for base course, and amplitude of temperature decrease within surface course on stress intensity factors at crack tip are presented in Figs. 4-8.

Figs. 4-8 indicate that surface course thickness has little effect on stress intensity factor at crack tip under thermal stresses, whereas modulus of surface course, coefficient of thermal contraction of surface course, coefficient of thermal contraction of base course, and amplitude of temperature decrease within surface course all have a significant effect stresses intensity factors.

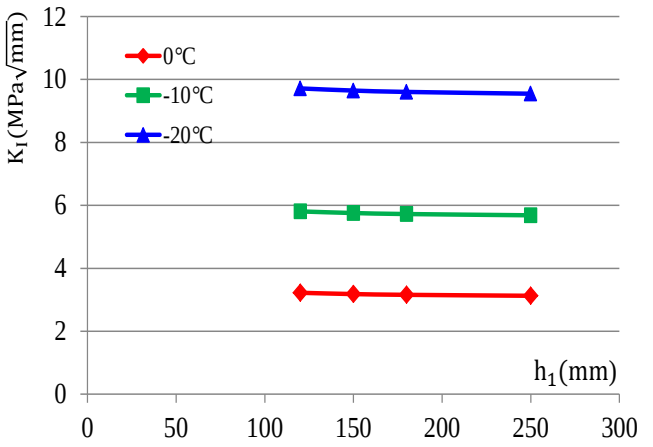

Fig. 4. Effects of Surface Course Thickness on Stress Intensity Factor.

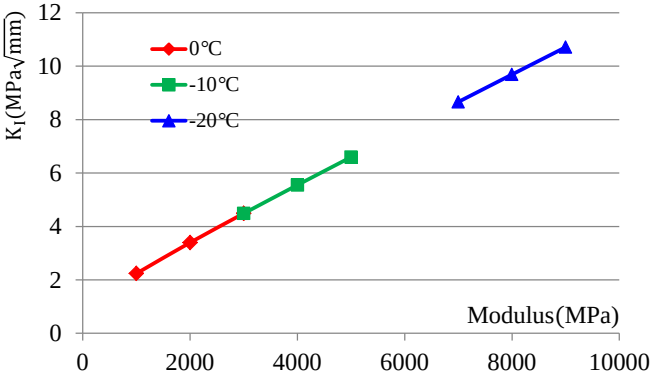

Fig. 5. Effects of Surface Course Modulus on Stress Intensity Factor.

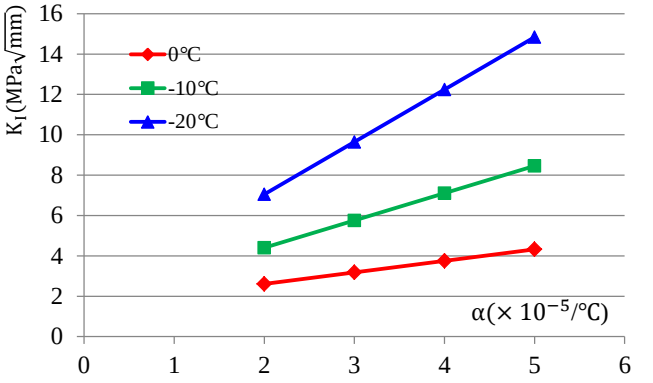

Fig. 6. Effects of Coefficient of Thermal Contraction of Surface Course on Stress Intensity Factor.

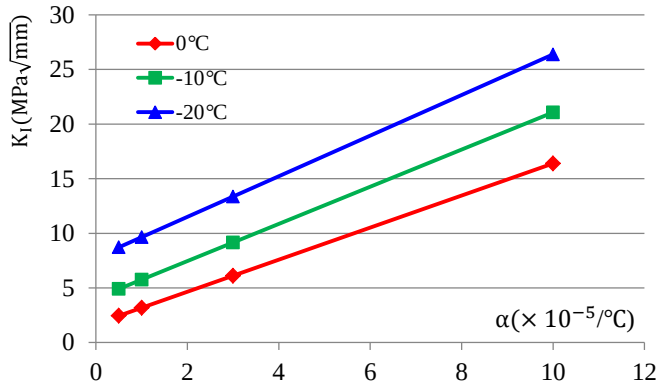

Fig. 7. Effects of Coefficient of Thermal Contraction of Base Course on Stress Intensity Factor.

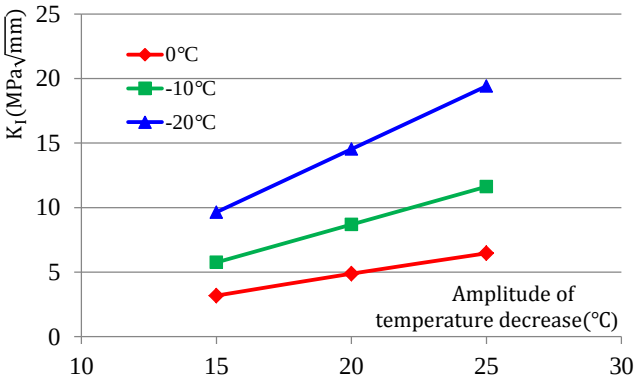

Fig. 8. Effects of Amplitude of Temperature Decrease in Surface Course on Stress Intensity Factor.

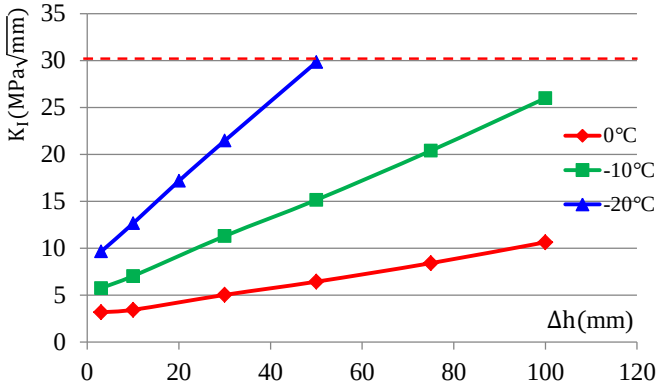

Fig. 9. Effects Crack Length within Surface Course on Stress Intensity Factor.

Crack Propagation within Surface Course

The stress intensity factor at crack tip will increase as the crack propagates from base course into surface course. This propagation can be divided into two stages: stable propagation before stress intensity factor reaches fracture toughness, and unstable propagation after fracture toughness is exceeded. As seen in Table 2, fracture toughness of 30MPa$\sqrt{mm}$ was selected as the threshold between stable and unstable crack propagation. Through FEM analysis on pavement structure as presented in Fig. 3, with parameters as shown in Tables 3 and 4, crack propagation within pavement structure is presented in Fig. 9. Fig. 9 indicates that the crack propagation is within the stable stage before it propagates 50mm into the surface course. Thereafter, it will enter unstable propagation stage under -20˚C. However, the crack propagation is still within stable stage even after the crack propagates 100mm into the surface course under 0˚C and -10˚C.

Summary and Conclusion

In this study, a new approach using refined regular elements was introduced to capture the stress singularity at crack tip. Fracture toughness results from three point bending beam tests were used to verify the effectiveness of this new refinement approach and it was found that this approach can effectively capture the stress singularity at crack tip. Sensitivity analysis was performed on stress intensity factor at crack tip to determine critical factors on surface course cracking behavior. Surface course thickness was found to have little effect on stress intensity factor at crack tip under thermal stress. Two stages, stable propagation and unstable propagation exist within the surface course crack propagation process. The lower the temperature, the shorter the crack length before it reaches the unstable crack propagation stage.

References

1. Scherocman, J. A., (1991). *International State-of-the-Art Colloquium on Low-Temperature Asphalt Pavement Cracking*, Special Report, U.S. Army Cold Regions Research and Engineering Laboratory, Hanover, NH, USA.
2. Marasteanu, M., Zofka, A., Turos, M., Li, X., Velasquez, R., Buttler, W., Paulino, G., Braham, A., Dave, E., Ojo, J., Bahia, H., Williams, C., Bausano, J., Gallistel, A., and McGraw, J. (2007). Investigation of Low Temperature Cracking in Asphalt: Pavements National Pooled Fund Study 776, Minnesota Department of Transportation, *MN/RC 2007-43*, St Paul, MN, USA.
3. Liu, C., Wu, S., and Wang, J. (2008). Investigation of the Low-Temperature Performance of Asphalt Mixtures via Fatigue and Linear Contraction and Creep Test, *Proc. SPIE 7375*, ICEM 2008: International Conference on Experimental Mechanics, 737511, Nanjing, China; doi:10.1117/12.839062.
4. Buttlar, W.G., Behnia, B., and Reis, H.M. (2011). Acoustic Emission-Based Test to Determine Asphalt Binder and Mixture Embrittlement Temperature, Final Report, University of Illinois at Urbana-Champaign , NCHRP-IDEA Project 144, IL, USA.
5. Das, P. (2009). Towards a Uniform Fracture Mechanics-Based Framework for Flexible Pavement Design, Master Thesis, Royal Institute of Technology SE-100 44, Stockholm, Sweden.
6. Henshell, R.D. and Shaw, K.G. (1975). Crack Tip Finite Elements Are Unnecessary, *International Journal for Numerical Methods in Engineering*, 9, pp. 495-507.
7. Barsoum, R.S. (1976). On the Use of Isoparametric Finite Elements in Linear Fracture Mechanics, *International Journal for Numerical Methods in Engineering*, 10, pp. 551-564.

8. Barsoum, R.S. (1977). Triangular Quarter-Point Elements as Elastic and Perfectly-Plastic Crack Tip Elements, *International Journal for Numerical Methods in Engineering*, 11, pp. 85-98.
9. MTPRC (2006). Specifications for Design of Highway Asphalt Pavement, Ministry of Transport of People's Republic of China JTG D50-2006, China Communications Press, Beijing, China (in Chinese).
10. Chen, C. (1978). *Research on Metal Fracture*, Metallurgical Industry Press, Beijing, China (in Chinese).
11. Wu, G. (1995). *Thermal Stress Analysis on Asphalt Pavement with Semirigid Base*, China Communications Press, Beijing, China (in Chinese).